Journal of Alloys and Compounds 408–412 (2006) 788–790

Journal of ALLOYS AND COMPOUNDS

www.elsevier.com/locate/jallcom

Variation of emission spectra of Er^{3+}-doped YAG-based solid solution

Masayuki Nishi[a,*], Setsuhisa Tanabe[b,1], Koji Fujita[a], Kazuyuki Hirao[a]

[a] *Department of Material Chemistry, Graduate School of Engineering, Kyoto University, Nishikyo-ku, Kyoto 615-8510, Japan*
[b] *Graduate School of Human and Environmental Studies, Kyoto University, Sakyo-ku, Kyoto 606-8501, Japan*

Received 31 July 2004; received in revised form 1 December 2004; accepted 7 December 2004
Available online 15 June 2005

Abstract

Er^{3+}-doped YAG crystal has intense emission bands in the U-band region (1625–1675 nm), which is uncommon to the $^4I_{13/2}$–$^4I_{15/2}$ transition of Er^{3+} in many hosts except for garnet type crystals. In order to seek the possibility to broaden the spectrum composed of many sharp bands, solid solutions based on $Y_3Al_5O_{12}$ (YAG) and $Ca_3Al_2(SiO_4)_3$ (CASG) crystals doped with Er^{3+} ions were prepared by solid-state reactions and their emission spectra in optical-telecommunication band were examined. Both of the YAG and CASG crystals have garnet type structures with similar lattice constants. The spectral linewidth dramatically increased with increasing CASG content, which promises to overcome the difficulty in the gain flatness for optical amplification in the wavelength-division-multiplexing (WDM) system. The line broadening can be attributed to the inhomogeneous distribution of the Er^{3+} sites achieved by the double substitutions of Si^{4+} for Al^{3+} in the tetrahedral site and of Ca^{2+} for the Y^{3+}.

Keywords: Disordered systems; Luminescence; Crystal and ligand fields

1. Introduction

Er^{3+}-doped fiber amplifiers (EDFAs) are used in the wavelength-division-multiplexing (WDM)-based optical telecommunication for the following reasons: the wavelength of the $^4I_{13/2}$–$^4I_{15/2}$ transition of Er^{3+} matches the minimum loss region of the silica-based optical telecommunication fiber and the quantum efficiency of the transition is usually very high even in oxide materials with high phonon energy. The EDFAs are generally used for the C-band (1530–1565 nm) and the L-band (1565–1625 nm) owing to their emission spectra in glass hosts [1–5]. In order to meet the growing demand for data capacity, the extension of the telecommunication band will be required [6,7]. The Er^{3+}-doped YAG crystal has the emission spectrum extending to the U-band (1625–1675 nm), owing to the characteristic large Stark splitting of both the initial $^4I_{13/2}$ and terminal $^4I_{15/2}$ levels [8,9]. An Er^{3+}-doped YAG (Er:YAG) precipitated glass–ceramic material can be an excellent candidate for optical amplifiers, especially in the U-band, since they would have optical properties of the Er:YAG and fiberizabilty of the glass materials; they can be transparent to the incoming signal light if the crystal size is much smaller than the wavelength [10–12]. Although the Er:YAG crystal itself can also be a candidate for optical amplifiers as planer wave-guide forms, the spectrum consists of many sharp bands, which causes the difficulty in gain flatness for amplification of signal lights with different wavelengths in the WDM system. In this report, solid solutions between $Y_3Al_5O_{12}$ (YAG) and $Ca_3Al_2(SiO_4)_3$ (CASG) were prepared in various molar ratios and the emission spectra were measured in order to seek the possibility to broaden the sharp bands. Relationship between the emission bandwidth and CASG content was investigated. CASG is chosen since both YAG and CASG have the garnet structure and the difference in lattice constant is ∼1%: the partial substitutions of Si^{4+} for Al^{3+} and Ca^{2+} for Y^{3+} in YAG will induce structural inhomogeneity around Er^{3+} so that the emission spectrum will be homogeneously broadened.

---

[*] Corresponding author. Tel.: +81 75 383 2418; fax: +81 75 383 2410.
E-mail addresses: west@collon1.kuic.kyoto-u.ac.jp (M. Nishi), stanabe@gls.mbox.media.kyoto-u.ac.jp (S. Tanabe).

[1] Tel.: +81 75 753 6832; fax: +81 75 753 6634.

0925-8388/$ – see front matter © 2005 Elsevier B.V. All rights reserved.
doi:10.1016/j.jallcom.2004.12.074

2. Experimental

The Er^{3+}-doped polycrystalline pellets were prepared from regent grade Y_2O_3, Al_2O_3, $CaCO_3$, SiO_2 and Er_2O_3. The raw materials were mixed thoroughly in the molar ratios of xYAG-$(10-x)$CASG ($x = 10$, 9, 8, 7 and 5) doped with 0.375 mol% of Er_2O_3 substituting Y_2O_3. The mixtures were pressed into pellets. The pellets were heated in an electrical furnace at a suitable temperature (=1350–1600 °C) for 6 h. The heat-treated pellets were crushed into powders and pressed into pellets, which were sintered again at the temperature for 6 h. This process was repeated at least twice.

X-ray powder diffraction (XRD) measurements were performed using a Cu Kα radiation (XRD-6000, Shimazu). For the analysis of the lattice constant, mixtures of samples and the 10–15 wt% standard silicon metal powders (325 mesh) were used for measurement; the diffraction angle 2θ was scanned from 10° to 80° in 0.02 increments with a scan speed of 0.5°/min. The lattice constant was obtained from the diffraction angle of the (420) peak of garnet crystal, which was determined by the difference from that of the (1 1 1) peak ($2\theta = 28.443°$) of the standard silicon.

Fluorescence spectra were measured in the range of 1380–1750 nm with a computer-controlled monochromator (Nikon, G-250), a PbS photodiode detector (Hamamatsu, P4638) and a lock-in-amplifier (NF Electronic Instruments, LI-570A). A diode laser of 970 nm (SDL-6362-P1) was used as the excitation source.

3. Results

The XRD patterns of the prepared crystals are shown in Fig. 1. All of the prepared crystals show the XRD patterns attributed to the YAG (JCPDS card No. 33-0040)-based garnet crystal. It was found that the diffraction peaks are shifted to the higher angle as the CASG content increases. Fig. 2 shows the compositional dependence of the lattice constants of the prepared garnet crystals. The solid line in the figure indicates the lattice constant expected by the Vegard's rule for ideal solid solutions; the value of a property is linearly interpolated from the endpoints of the composition range. The lattice constants almost linearly decreased with increasing CASG content, and the deviation from the Vegard's rule was observed. The emission spectra of the $^4I_{13/2}$–$^4I_{15/2}$ transition of Er^{3+} are shown in Fig. 3. In the figure, the possible emission wavelengths of the transition of Er^{3+} in YAG crystal are also shown as bars, which are calculated by the Stark splitting of both the $^4I_{13/2}$ and $^4I_{15/2}$ levels [8]. All of the emission spectra can be attributed to the $^4I_{13/2}$–$^4I_{15/2}$ transition of Er^{3+} in YAG-based garnet crystals. The increase in the emission linewidth was also observed with increase in the CASG content.

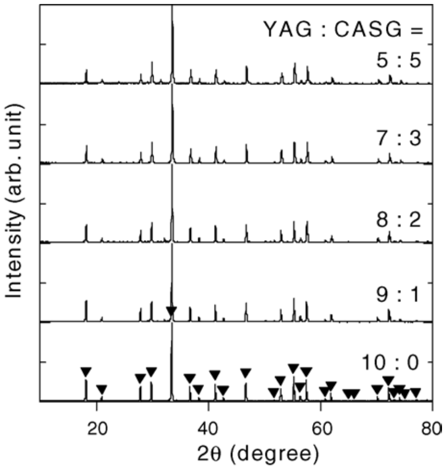

Fig. 1. XRD patterns of the prepared crystals with molar ratios of xYAG-$(10-x)$CASG ($x = 10$, 9, 8, 7 and 5) doped with 0.375 mol% of Er_2O_3 instead of Y_2O_3.

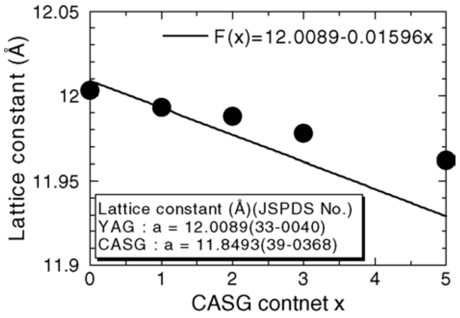

Fig. 2. The compositional dependence of the lattice constants of the prepared YAG-based garnet solid solutions. The solid line in the figure indicates the lattice constant expected by Vegard's rule for ideal solid solutions.

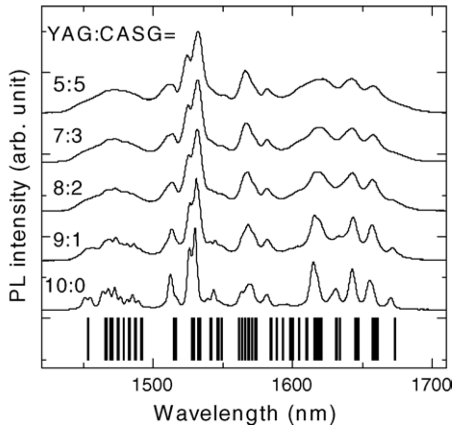

Fig. 3. The fluorescence spectra of the $^4I_{13/2}$–$^4I_{15/2}$ transition of the Er^{3+} in the prepared YAG-based garnet solid solutions. The finger pattern denotes the possible emission wavelengths calculated using the values of Stark splitting of the $^4I_{13/2}$ and $^4I_{15/2}$ levels of Er^{3+} in YAG crystal [8].

4. Discussion

The lattice constants reported in JSPDS cards are 12.0089 Å for YAG and 11.8493 Å for CASG, respectively.

The almost linear decrease in the lattice constants with increasing CASG content indicates that the solid solutions between YAG and CASG are successfully prepared. Since the Vegard's rule is only applied to the ideal homogeneous solid solutions, the deviation from the rule can occur even for the homogeneous solid solution and can also occur for the heterogeneous solid solution and for the solid solution with impurity phases; however, the determination of the dominant origin of the deviation calls for further investigation.

The large broadening of the emission linewidth of Er^{3+} in the solid solutions can be interpreted from the viewpoint of the inhomogeneity in the local environment around Er^{3+} caused by the cation substitutions. Since both Er^{3+} and Y^{3+} have the trivalent state and the difference in ionic radii is less than 1%, both ions occupy the almost identical sites in a given crystal structure. In the YAG crystal, the Er^{3+} occupies the Y^{3+} site with D_2 point symmetry surrounded by eight oxygens; the nearest-neighbor cations are four $Y^{3+}(8)$ ions at ∼3.68 Å from the Er^{3+}, four $Al^{3+}(6)$ ions at ∼3.36 Å and six $Al^{3+}(4)$ ions, two of which are at ∼3.00 Å and others are at ∼3.68 Å; the number in the parentheses is the oxygen coordination number of the cation in the given site [13]. In the YAG-based garnet solid solution, the Si^{4+} and Ca^{2+} ions occupy the $Al^{3+}(4)$ and $Y^{3+}(8)$ sites, respectively, because of their ionic radii and occupying sites in the CASG crystal. The substitutions give large variations of the coordination environments around Er^{3+}. (If we assume fully random substitutions for the nearest cation polyhedron as described above irrespective of requirement of electroneutrality, 288 sites are expected for Er^{3+}.) The distribution of the site occupation probabilities changes with the molar ratio of CASG to YAG, and the number of the variations of the Er^{3+} site with countable relative probability increases with increasing CASG content, which contributes to the inhomogeneous distribution of the energy states of Er^{3+}, i.e., the inhomogeneous broadening of the emission linewidth. The substitutions of Ca^{2+} for $Y^{3+}(8)$ and of Si^{4+} for $Al^{3+}(4)$ induce the change in the electrondonating ability of oxide ions and the distances between the cations and oxygen ions, which can change the ligand fields around Er^{3+} and often lower the site symmetry. Since, in the solid solutions between YAG and CASG, Er^{3+} remains in the eight-coordinated site of the garnet type structure, the change in the ligand fields modifies the energy states of Er^{3+} as weak perturbation; therefore, the emission linewidth of Er^{3+} in the solid solution becomes broader with the feature of the spectral shape of Er:YAG crystal maintained depending on the increase in CASG content as is shown in Fig. 3.

5. Conclusions

In the solid solutions between the YAG and CASG crystals the spectral linewidth of the ${}^4I_{13/2}$–${}^4I_{15/2}$ transition dramatically increased as the CASG content increases. This line broadening is mainly attributable to the inhomogeneous broadening derived from increase in variation of Er^{3+} sites with different ligand field by substitutions of Si^{4+} for $Al^{3+}(4)$ and Ca^{2+} for $Y^{3+}(8)$. The line broadening in the solid solutions between YAG and CASG crystals can overcome the difficulty in the gain flatness of Er:YAG for optical amplification in the WDM system.

References

[1] C.A. Millar, M.C. Brierley, P.W. France, Proceedings of ECOC'88, part 1, 1988, p. 66.
[2] C.G. Atkins, J.F. Massicott, J.R. Armitage, R. Wyate, B.J. Ainslie, S.P. Craig-Ryan, Electron. Lett. 25 (14) (1989) 910.
[3] M. Yamada, M. Shimizu, M. Okayasu, T. Takeshita, M. Horiguchi, Y. Tachikawa, E. Sugita, IEEE Photonics Technol. Lett. 2 (3) (1990) 205.
[4] M. Yamada, M. Shimizu, M. Horiguchi, M. Okayasu, E. Sugita, IEEE Photonics Technol. Lett. 2 (9) (1990) 656.
[5] A. Mori, Y. Ohishi, M. Yamada, H. Ono, Y. Nishida, K. Oikawa, S. Sudo, OFC'97 (1997) PD1.
[6] Y.G. Choi, K.H. Kim, B.J. Park, J. Heo, Appl. Phys. Lett. 78 (9) (2001) 1249.
[7] T.H. Lee, J. Heo, Y.G. Choi, B.J. Park, K.H. Kim, Chem. Phys. Lett. 384 (2004) 16 (Abstract).
[8] A.A. Kaminskii, Crystalline Lasers: Physical Processes and Operating Schemes, CRC Press, New York, 1996, p. 188, (Chapter 2).
[9] M. Nishi, S. Tanabe, K. Fujita, K. Hirao, in: J. Mørk, A. Srivastava (Eds.), OSA Trends in optics and photonics (TOPS) vol. 92, Optical amplifiers and their applications, 2003, p. 45.
[10] P.A. Tick, N.F. Borrelli, L.K. Cornelius, M.A. Newhouse, J. Appl. Phys. 78 (11) (1995) 6367.
[11] P.A. Tick, Opt. Lett. 23 (24) (1998) 1904.
[12] M.J. Dejneka, J. Non-Cryst. Solids 239 (1998) 149.
[13] R.W.G. Wyckoff, Crystal Structures, vol. 3, Interscience Publishers, New York, 1965, p. 222, (Chapter VIIIC).